

# Symbiotic stars in X-rays II: faint sources detected with XMM-Newton and Chandra.

N. E. Nuñez,<sup>1</sup> G. J. M. Luna,<sup>2</sup> I. Pillitteri<sup>3</sup> and K. Mukai<sup>4</sup>

<sup>1</sup> Instituto de Ciencias Astronómicas de la Tierra y el Espacio (ICATE-UNSJ), Av. España (sur) 1512, San Juan - Argentina  
e-mail: nnunez@icate-conicet.gob.ar

<sup>2</sup> Instituto de Astronomía y Física del Espacio (IAFE), CC 67 - Suc. 28 (C1428ZAA) CABA - Argentina.

<sup>3</sup> Osservatorio Astronomico di Palermo (INAF), Piazza del Parlamento 1, 90 134 Palermo - Italy.

<sup>4</sup> CRESST and X-ray Astrophysics Laboratory, NASA/GCFC, Greenbelt, MD 20 771 - USA. Department of Physics, University of Maryland, Baltimore County, 1 000 Hilltop Circle, Baltimore, MD 21 250 - USA.

## ABSTRACT

We report the detection, with *Chandra* and XMM-Newton, of faint, soft X-ray emission from four symbiotic stars that were not known to be X-ray sources. These four object show a  $\beta$ -type X-ray spectrum, i.e. their spectra can be modeled with an absorbed optically thin thermal emission with temperatures of a few million degrees. Photometric series obtained with the Optical Monitor on board XMM-Newton from V2416 Sgr and NSV 25735 support the proposed scenario where the X-ray emission is produced in a shock-heated region inside the symbiotic nebulae.

**Key words.** binaries: symbiotic, X-rays: individuals: Hen 2-87, NSV 25735, V2416 Sgr and Hen 2-104

## 1. Introduction

In a binary system where a white dwarf (WD) accretes from the wind of a red giant companion and frequently forms an accretion disk; where the WD can experiences frequent outburst of different intensity and where mass is ejected at speeds of a few hundreds  $\text{km s}^{-1}$ , it seems natural to expect that X-ray emission could be frequently detected, originated either in the surface of the white dwarf by quasi-stable nuclear burning, in the accretion disk, or in shocks due to ejections of material. However, it was only recently that a significant fraction of these systems, known as WD symbiotics, was detected at X-ray wavelengths using modern instruments such as *Swift*, XMM-Newton or *Chandra*. In general, the emission is faint, with fluxes as low as a few  $10^{-14} \text{ ergs cm}^{-2} \text{ s}^{-1}$ . WD symbiotics have X-ray spectra that can be classified into four types: supersoft X-ray sources whose X-ray spectrum peaks at energies lower than 0.4 keV, named  $\alpha$ -type;  $\beta$ -type comprises those sources with soft X-ray emission and whose spectrum extends up to energies of less than 2.4 keV;  $\delta$ -type are highly absorbed, hard X-ray sources with detectable thermal emission above 2.4 keV and  $\beta/\delta$ -type includes those WD symbiotics with two X-ray thermal components, soft and hard (this classification scheme is detailed in Luna et al. 2013, hereafter Paper I).

In this paper we present the detection at X-ray energies of four WD symbiotics: Hen 2-87, NSV 25735, V2416 Sgr and Hen 2-104 observed with XMM-Newton and *Chandra* that were not known to be X-ray sources before. In Section 2 we detailed the data reduction while in Section 3 we present the results, while discussion and concluding remarks are presented in Section 4.

## 2. Observations and data reductions

We searched for imaging X-ray observations sensitive in the 0.3-10 keV band (*ASCA*, XMM-Newton, *Chandra*, *Suzaku* and *Swift*) using the HEASARC<sup>1</sup> database of all the symbiotic stars listed in (Belczyński et al. 2000). Excluding the symbiotic stars already known to be X-ray sources (see Paper I which contains a complete list of known X-ray emitting symbiotic stars), we detected X-ray emission from four symbiotic stars: Hen 2-87, NSV 25735, V2416 Sgr and Hen 2-104.

Hen 2-87, NSV 25735 and V2416 Sgr were observed with XMM-Newton. While NSV 25735 and V2416 Sgr were the main target of the observations, Hen 2-87 was serendipitously detected at the edge of the field of view of the EPIC camera, about  $10''$  away from the aim point. The XMM-Newton data were re-processed using the SAS (v13.0.1) tool `emproc` and `epproc` to apply the latest calibration. All observations were obtained in full mode and with the thick filter. After filtering the event list for flaring particle background, Hen 2-87 and V2416 Sgr were evidently detected and we extracted source spectra and light curves from circular regions centered on the SIMBAD coordinates of each objects with radius of 600 or 640 pixels ( $\sim 32''$ ) (we used an smaller region in the case of Hen 2-87 because it lies close to a detector edge). Ancillary and response matrices were created with the SAS tools `arfgen` and `texttrmgen`. The background spectra and light curves of NSV 25735 and V2416 Sgr were extracted from annuli regions centered on the source with inner and outer radii of 650 and 1 000 pixels, respectively. Because Hen 2-87 is located near the detector edge, we extracted the background from a circle off-centered from the source region with  $90''$  radius. Given the faintness of the sources, we combined the *pn*, *mos1* and *mos2* spectra (using the `epicspeccombine` script) increasing the signal-to-noise of the spectra to be modeled.

**Table 1.** Observations Log

Object	Instrument	ObsID	Date	Exposure time [ks]	Offset["] <sup>1</sup>
Hen 2-87	XMM-Newton - EPIC	0109480101	2 002/06/03	53	10.402
		0109480201	2 002/08/26	55	10.402
		0109480401	2 003/01/21	48	10.403
NSV 25735	XMM-Newton - EPIC	0401670201	2 007/04/30	10	0.007
V2416 Sgr	XMM-Newton - EPIC	0099760201	2 000/03/22	61	0.005
	XMM-Newton - OM	0099760201	2 000/03/22	47	0.005
Hen 2-104	Chandra - ACIS	2577	2 002/04/08	20	0.022

To search for X-ray emission from NSV 25735, we used an algorithm based on wavelet convolution for the EPIC XMM-Newton images. This code is derived from the *ROSAT* and *Chandra* versions (see Damiani et al. 1997a and Damiani et al. 1997b for details). The XMM-Newton version allows to perform source detection on the data of the three EPIC camera simultaneously, improving thus the sensitivity of the result. The detected sources are those with a significance threshold higher than  $4.5\sigma$  of the local background. This threshold is chosen on the basis of simulations of background only images, in order to retain at most one spurious source in the image. NSV 25735 is detected at a significance level of  $15.22\sigma$ , it has about  $400\pm40$  counts in the sum of *pn*, *mos1* and *mos2* images and a rate of  $\sim 12$  counts  $s^{-1}$ .

NSV 25735 and V2416 Sgr were also observed with the optical monitor (OM) onboard XMM-Newton. While NSV 25735 was observed in fast imaging mode with the UVM2 filter, V2416 Sgr was observed in image mode using the U, B and V filters (UVW2 and UVM2 filters were also used but the data were corrupted). We analyzed pipeline-reduced data and look for variability in the photometric time series. NSV 25735 has been observed with *Swift*/XRT/UVOT, however, the source was not detected in X-rays and the UVOT images were saturated (see Paper I for details).

Hen 2-104 was observed with *Chandra* using the ACIS-S camera. We reprocessed the data using the `chandra_repro` script in CIAO<sup>2</sup> and obtained a new event file with the calibration version 4.5.2 applied. Afterwards, we extracted spectra (using the `specextract` script) and light curves (using the `dmextract` script) for the source and background. Source products were extracted from a circular region (centered on the SIMBAD<sup>3</sup> coordinates) with 100 pixels ( $\sim 50''$ ) radius while background spectra and light curves were extracted from 3 circular regions of 160 pixels ( $\sim 80''$ ) each. The response and ancillary matrices were created using the `mkrmf` and `mkarf` scripts. All the observations are detailed in Table 1.

We fit the unbinned spectra using XSPEC<sup>4</sup> and because it is not appropriate to use the  $\chi^2$  statistic to fit the spectra of sources with a low numbers of counts, such as the ones studied here, we use the C-statistic (Cash 1979). All errors in the fit parameters were estimated at their 90% confidence. To evaluate how many components are needed in the spectral model, we use the likelihood ratio test as described by Protassov et al. (2002) and implemented in XSPEC through the `lrt` script. This test compares the statistics (Cstat) of the complex and simple model in  $N$  sets of simulated data and helps us to evaluate how statistically significant is to add one or more components into a single-component model.

### 3. Results

By correlating the existing catalogue of Belczyński et al. (2000) with the HEASARC database, we found X-ray emission from four symbiotic stars observed with XMM-Newton and *Chandra*. Their low X-ray fluxes (see Table 2) explain why these sources were not detected before. Given the limited statistical quality of these X-ray data, we limit ourselves to spectral models that have been successfully used for other symbiotic stars. All of them show a soft optically thin thermal X-ray spectrum with emission that peaks around 1 keV and do not extend to very high energies. This is sufficient to fit their spectra and classify them as  $\beta$ -type in the scheme detailed in Paper I (in the next subsections we detail the fit procedure for each object). We also tried to fit the X-ray spectrum with non-thermal models which were discarded because they yielded unrealistic values for the fit parameters.

For all sources, we show the classification based on infrared (IR) colors proposed by Webster & Allen (1975) and refined by Allen (1984), where *S*-type systems emit IR radiation typical of red giant atmospheres (*M*-type), they are relatively dust-free and have binary periods shorter than 20 years; *D*-type systems show IR emission indicative of dust, that is, thermal radiation with average temperatures of 1 000 K, generally contain Mira variables as companions and have binary periods longer than 10 years like R Aqr who show a period of 46 years (Gromadzki & Mikołajewska 2009). *D'*-type systems have very red colors in the far IR and a cool companion of spectral types F or G. The IR type of all objects was extracted from Table 1 in Belczyński et al. (2000).

#### 3.1. Hen 2-87

This object is classified as *S*-type. Little is known about this source and there are not recorded outburst in the literature. Hen 2-87 was detected in three XMM-Newton observations in the field of WR 47 (see Table 1). Given that the source was detected at a higher count rate during ObsID 0109480401 (hereafter 401) taken in 2003 ( $0.037\pm0.001 s^{-1}$ , compared to  $0.011\pm0.002$  counts  $s^{-1}$  during ObsID 0109480201 (hereafter 201) and  $0.013\pm0.002$  counts  $s^{-1}$  for ObsID 0109480101 (hereafter 101)), we fit this spectrum and then used the accepted model to fit the other two datasets. We first fit the spectrum with an absorbed optically thin thermal plasma (`wabs*apec`) but there were important residuals in the  $E \gtrsim 2$  keV region. Then, we added a second optically thin thermal component, also affected by the same absorber than the previous component (`wabs*(apec1+apec2)`), and the fit showed a much more uniform distribution of the residuals. As explained in Section 2, we used the `lrt` to assess the statistical significance of adding this second component and after 1 000 simulations, 60% of them showed an improvement in the statistic. The addition of the second component has a low significance, however given that this component describe the high energy part of the spectrum, we

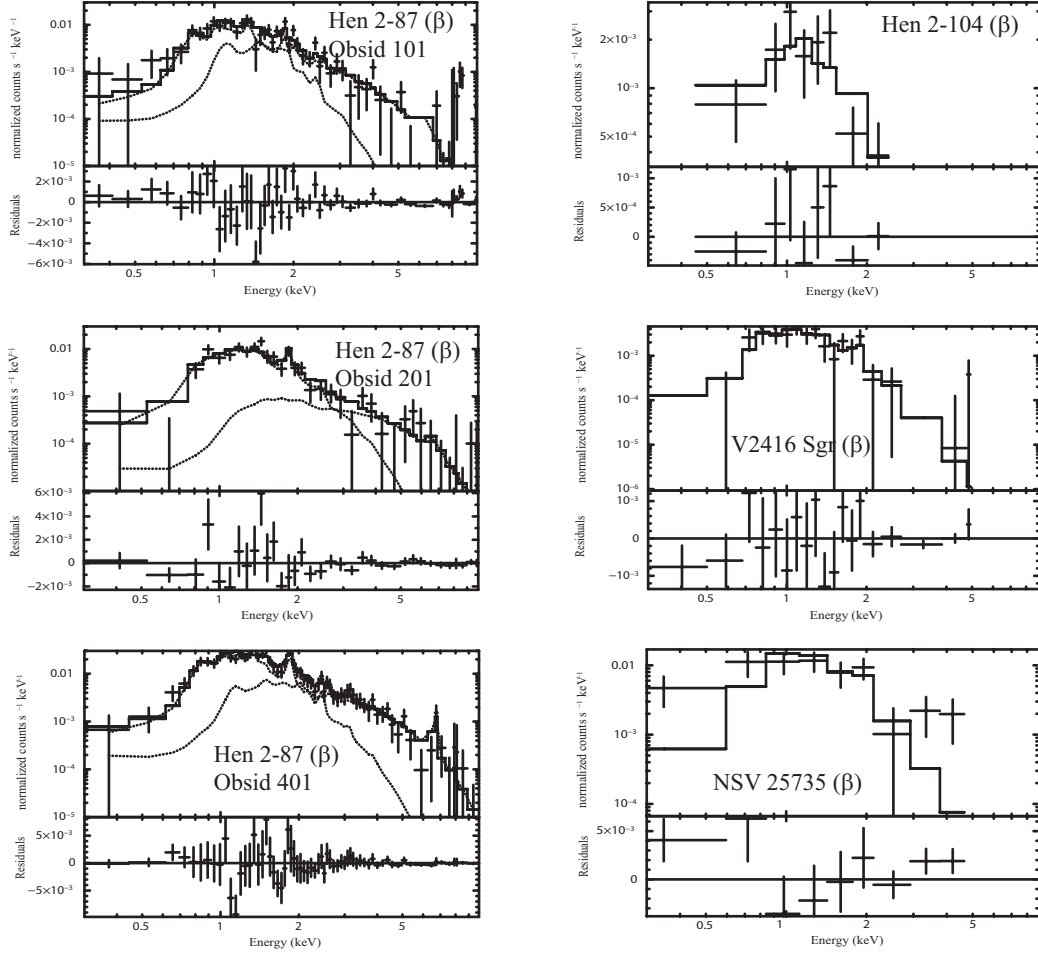


**Fig. 1.** *Chandra* and *XMM-Newton* X-ray spectra of the WD symbiotic with newly discovered X-ray emission together with their X-ray spectral types: Hen 2-87, Hen 2-104, V2416 Sgr and NSV 25735. We show the 3 spectra obtained with *XMM-Newton* from Hen 2-87. The full line shows the best-fit model described in Section 3, while the dotted line shows the contribution of the individual spectral components in the case of multi-component models. The X-ray spectral classification for each source is included between parentheses in each panel.

find plausible to keep it in our model (see Fig. 3). We retain this complex model throughout the analysis, which could be better tested in more sensitive observations. During the 3 observations, the plasma temperatures and the absorbing column have commensurate values. The flux on the other hand, almost doubled from ObsID 101 to 401 (see Table 2).

### 3.2. NSV 25735

The symbiotic NSV 25735 is classified as  $D'$ -type. The system contains a WD with moderate temperature ( $T \sim 50\,000$  K, Schmid & Nussbaumer 1993). The cool companion star has three different spectral type determination in the literature: G5 (Mürset & Schmid 1999), G4 III/IV (Smith et al. 2001), and G7 III (Munari et al. 2001) suggesting a  $T_{\text{eff}}$  in a range between 5 025–5 300 K. The cool component is rotating at a spectacular speed of  $105 \text{ km s}^{-1}$ , unseen in field G-type giants (Munari et al. 2001). As only 7  $D'$ -type symbiotic are known, the fact that the 3 sources (HD 330036, AS 201 and NSV 25735) studied so far with high resolution optical spectroscopy show rapid rotation and  $s$ -process elemental overabundances, might indicate that these two traits are signatures of these symbiotic systems (Jorissen et al. 2005). Moreover, NSV 25735 is the first  $D'$ -type symbiotic to show jets. Munari et al. (2001) analyzed the H $\alpha$

profile and found a central component (that remained constant for months) and two weaker and symmetrically placed components at both sides of the profile. These two components show large day-to-day variability (velocity and width), which are spectral signatures of jet-like discrete ejection events. Also, the authors derived a high orbital inclination of  $60^\circ$ , therefore the de-projected velocity of the jet components must be much larger than the observed velocity shifts ( $150 \text{ km s}^{-1}$ ) and well in excess of the escape velocity from the companion ( $1\,000 \text{ km s}^{-1}$ ). The jet components are visible in the profiles of He I lines as well, with a velocity of  $300 \text{ km s}^{-1}$ . There are not recorded outbursts but the bipolar mass outflow is highly variable (Munari et al. 2001). The very fast rotation has been explained by Jeffries & Stevens (1996), who proposed a mechanism in which the accretion of a slow massive wind from the AGB progenitor of the current WD can transfer sufficient angular momentum, spinning up the companion, in analogy with millisecond radio pulsars (van den Heuvel & Bonsema 1984). This also explains the chemical enrichment in  $s$ -process elements in  $D'$ -type symbiotic systems that were present in the AGB wind (Pereira et al. 2005).

The X-ray spectrum obtained with *XMM-Newton*, that extends up to energies of  $\sim 5 \text{ keV}$ , can be modeled using an absorbed ( $N_H = 1.2^{+0.4}_{-0.4} \times 10^{22} \text{ cm}^{-2}$ ) optically thin thermal plasma with a temperature  $kT = 0.7^{+0.3}_{-0.3} \text{ keV}$ . *XMM-Newton* detected

351 source counts, therefore the model parameters cannot be constrained by the fit (see Table 2). The unabsorbed flux in the 0.3-10.0 keV energy band is  $F_X = 9^{+3}_{-3} \times 10^{-13}$  ergs cm<sup>-2</sup> s<sup>-1</sup> and the corresponding luminosity at a distance of 575 pc (Munari et al. 2001) is  $L_X = 3^{+2}_{-1} \times 10^{31}$  ergs s<sup>-1</sup>.

### 3.3. V2416 Sgr

This object was classified as a *S*-type symbiotic. XMM-Newton detected 220 counts from this source. The X-ray spectrum can be modeled with an absorbed ( $N_H = 1.1^{+0.3}_{-0.2} \times 10^{22}$  cm<sup>-2</sup>) optically thin thermal plasma (with  $kT = 0.5^{+0.2}_{-0.2}$  keV). It is interesting to note that the value of  $N_H$  that could be inferred (using the relation between  $N_H$  and  $E(B-V)$  proposed by Groenewegen & Lamers 1989) from the published reddening values of  $E(B-V) = 1.7$  is  $4.4 \times 10^{22}$  cm<sup>-2</sup> (Luna & Costa 2005) or using  $E(B-V) = 2.5$  (Mikolajewska et al. 1997) we have  $N_H = 6.6 \times 10^{22}$  cm<sup>-2</sup>. Both values are much higher than the value found from our fit of the X-ray spectrum. On the other hand, Whitelock & Munari (1992), calculated a lower value of  $E(B-V) \sim 0.13$ , but at the same time they mentioned that the colors of this star suggest it experiences several magnitude more extinction than the value derived. This suggest that the X-ray emitting region could be located in the outer parts of the symbiotic nebulae, where column density is smaller and so is the absorption. The unabsorbed flux in the 0.3-10.0 keV energy band is  $F_X = 0.9^{+0.2}_{-0.2} \times 10^{-13}$  ergs cm<sup>-2</sup> s<sup>-1</sup> and the corresponding luminosity at a distance of 1.0 kpc (the actual distance is unknown) is  $L_X = 1.0^{+0.2}_{-0.2} \times 10^{31}$  ergs s<sup>-1</sup>.

The OM light curves from V2416 Sgr and NSV 25735 show a small fractional variability  $\lesssim 3\%$  (which we calculate as the observed variance over the average count rate), which is expected for their  $\beta$  X-ray spectral type. In the diagram presented in Paper I (Fig. 7), where the hardness of the X-ray spectrum is plotted against the fractional UV variability, it can be clearly seen a separation between those systems that are accretion-powered and those that are powered by quasi-stable shell burning. NSV 25735 and V2416 Sgr are located in the lower left corner, in the region of systems where the WDs are powered by quasi-stable shell burning.

### 3.4. Hen 2-104

Hen 2-104 is classified as a *D*-type symbiotic. Its extended nebula has an hourglass shape, extending 75'' (Schwarz et al. 1989). More detailed studies showed that the nebula around Hen 2-104 consists in nested hourglass-shaped structures (with the inner structure extending  $\sim 12''$  while the outer structure extends for  $\sim 80''$ ) and a collimated polar jet (see Fig.1 in Corradi et al. 2001). The outer pair of lobes and jets are produced by a high-velocity outflow from the WD companion of the Mira, while the inner, slowly expanding lobes are produced by the Mira wind itself (Corradi et al. 2001). The densities range from  $n_e = 500$  cm<sup>-3</sup> to 1 000 cm<sup>-3</sup> in the inner lobes, and from 300 cm<sup>-3</sup> to 500 cm<sup>-3</sup> in the outer lobes (Santander-García et al. 2008).

The *Chandra* observation was already studied by Montez et al. (2006), although due to poor astrometry, they mistakenly attributed the X-ray emission to a region heated by shocks and displaced 2'' SE from the central symbiotic system (R. Montez private communication). Our new data analysis shows that the X-ray emission is concentrated in the central region of the nebula. The faint X-ray emission can be modeled with an absorbed ( $N_H \lesssim 0.3 \times 10^{22}$  cm<sup>-2</sup>) optically thin thermal plasma (with  $kT \gtrsim 1.5$  keV), however, due to the low number of counts detected

(42) we are not able to constrain further the value of the model parameters, upper or lower limits are listed in Table 2. The unabsorbed flux in the 0.3-10.0 keV energy band is  $F_X = 0.3^{+0.1}_{-0.1} \times 10^{-13}$  ergs cm<sup>-2</sup> s<sup>-1</sup> and the corresponding luminosity at a distance of 3.3 kpc (Santander-García et al. 2008) is  $L_X = 4.2^{+1.0}_{-1.5} \times 10^{31}$  ergs s<sup>-1</sup>.

## 4. Discussion and conclusions

We found X-ray emission from four WD symbiotic that were not known to be X-ray sources. The X-ray emission from all of them can be classified as  $\beta$ -type, following the scheme originally proposed by Müerset et al. (1997) and recently updated in Paper I. Our results confirm that  $\beta$ -type X-ray emission is the most frequent among WD symbiotic, increasing the number of known  $\beta$ -type sources to 16 out of 48 symbiotic with X-ray emission. The X-ray emission from the new sources is faint, with luminosities on average of  $10^{31}$  ergs s<sup>-1</sup> (albeit the uncertainties in their distance), which explains why pointing, dedicated observations were necessary for their detection. As  $\beta$ -type systems, their X-ray emission seems to be associated with shocks in the nebulae that could be originated in a colliding wind region or inside extended jets (known to be present in NSV 25735 and Hen 2-104).

Although most models of colliding-wind scenarios require that the WD in the system underwent a recent outburst to be able to trigger a fast, tenuous wind, the  $\beta$ -type systems presented here as well as those presented in Paper I do not have any recent outburst recorded. While  $\alpha$  or  $\delta$  type X-ray spectra are directly linked to the source that powers the WD, i.e. shell-burning or accretion,  $\beta$  type X-ray emission is not. The absence of strong variability, together with a  $\beta$ -type X-ray spectrum strongly suggest that the observed X-rays are not originated in the accretion disk around the WD, while at the same time, those soft X-rays are too energetic to be originated in a shell-burning white dwarf. Our physical picture is that, in these systems, nuclear burning could lead to a strong wind from the WD (or the accretion disk near the WD), which collides with the wind from the cool star, leading to observed soft X-ray emission. Super-soft X-ray emission from the WD might be present as well but absorbed by the dense symbiotic nebula.

Using the temperature obtained from spectral models of these sources (0.4 keV to  $\sim 2.0$  keV) and assuming strong shock conditions, we can derive a shock speed,  $v_{shock}$ . We obtain  $v_{shock}$  in the range of  $\sim 1\,000$  to  $\sim 2\,500$  km s<sup>-1</sup>. Similar speeds are observed in the  $\beta$ -type sources presented in Paper I and Müerset et al. (1997) and are roughly consistent with the speeds of X-ray emitting outflows from WD symbiotic (Nichols et al. 2007; Galloway & Sokoloski 2004). High outflow speeds of a few thousands km s<sup>-1</sup> have been observed in the optical line profiles of MWC 560 (Schmid et al. 2001), although they are not consistent with the temperatures observed from the  $\beta$  component in its X-ray spectrum (Stute & Sahai 2009). The disparity between X-ray inferred speed and speeds from optical line widths has been also observed in the diffuse X-ray emission from planetary nebulae (Soker & Kastner 2003). In the dense symbiotic nebula, however, some authors have modeled the observed UV line profiles of O VI and He II as due to electron scattering (Sekeráš & Skopal 2012a,b). Lee (2000) proposed that Ramman scattering might be responsible for the broad H $\alpha$  line wings observed in symbiotics.

The number of known symbiotic with X-ray emission is rapidly increasing with the new instruments available and it is expected to increase even more with much sensitive instru-

**Table 2.** X-ray spectral fitting results. X-ray flux ( $F_X$ ) and luminosity ( $L_X$ ), in units of  $10^{-13}$  ergs s $^{-1}$  cm $^{-2}$  and  $10^{31}$  ergs s $^{-1}$  respectively, are calculated in the 0.3–10.0 keV energy band.

Object	Model	kT [keV]	$N_H$ [ $10^{22}$ cm $^{-2}$ ]	$F_X$	$L_X$
Hen 2-87(101)	wabs×(apec $_1$ +apec $_2$ )	1: $0.4^{+0.4}_{-0.2}$ 2: $1.9^{+0.9}_{-0.1}$	$1.3^{+0.2}_{-0.2}$	$7.5^{+0.9}_{-0.9}$	$9.0^{+0.7}_{-0.7}$
Hen 2-87(201)	wabs×(apec $_1$ +apec $_2$ )	1: $0.7^{+0.3}_{-0.1}$ 2: $\geq 2.0$	$1.2^{+0.2}_{-0.2}$	$8.1^{+1.1}_{-1.1}$	$9.7^{+1.3}_{-1.3}$
Hen 2-87(401)	wabs×(apec $_1$ +apec $_2$ )	1: $0.6^{+0.1}_{-0.1}$ 2: $3.0^{+1.0}_{-1.0}$	$1.4^{+0.1}_{-0.1}$	$14^{+1}_{-1}$	$20.0^{+2.2}_{-4.4}$
NSV 25735	wabs×apec	$0.7^{+0.3}_{-0.3}$	$1.2^{+0.4}_{-0.4}$	$9^{+3}_{-3}$	$3^{+2}_{-1}$
V2416 Sgr	wabs×apec	$0.5^{+0.2}_{-0.2}$	$1.1^{+0.3}_{-0.2}$	$0.9^{+0.2}_{-0.2}$	$1.1^{+0.2}_{-0.3}$
Hen 2-104	wabs×apec	$\geq 1.5$	$\leq 0.3$	$0.3^{+0.1}_{-0.1}$	$4.2^{+1.0}_{-1.5}$

ments and deeper surveys (e.g. *NuSTAR*<sup>5</sup> and *eROSITA*<sup>6</sup>). We now know 48 systems with X-ray emission originating in four different scenarios. With this number of sources it seems timely to study their statistical properties. Is there any trend or relationship between IR and X-ray spectral types? In the symbiotic stars catalog of Belczyński et al. (2000), 63 % of the objects (139) are classified as *S*-type, 15% (34) as *D*-type, and 3% (7) as *D'*-type. Among the 48 symbiotic with X-ray emission, 33% of them have a  $\beta$ -type X-ray spectrum. Roughly half of the  $\beta$ -type symbiotics have infrared *S*-type spectrum, while 25% have *D*-type, 6.3% have *D'*-type and 6.3% do not have classification. We did not find any clear tendency or correlation between IR and X-ray types, i.e. the fractions of IR types are roughly similar among X-rays emitting symbiotics and those with no X-ray emission detected.

**Acknowledgements.** We thank Jennifer L. Sokoloski for useful discussions about X-ray emission from symbiotic stars. N. E. N. acknowledge Consejo Nacional de Investigaciones Científicas y Técnicas, Argentina (CONICET) by the Postdoctoral Fellowship. G. J. M. Luna acknowledge funding from grants PICT/2011/269 from Agencia and PIP D-4598/2012 from Consensus National de Investigación Científicas y Técnicas, Argentina. This research has made use of data obtained from the High Energy Astrophysics Science Archive Research Center (HEASARC), provided by NASA's Goddard Space Flight Center; and the VizieR catalogue access tool, CDS, Strasbourg, France. The original description of the VizieR service was published in Ochsenein et al. (2000).

## References

- Allen, D. A. 1984, *Proceedings of the Astronomical Society of Australia*, 5, 369  
 Belczyński, K., Mikołajewska, J., Munari, U., Ivison, R. J., & Friedjung, M. 2000, *A&AS*, 146, 407  
 Cash, W. 1979, *ApJ*, 228, 939  
 Corradi, R. L. M., Livio, M., Balick, B., Munari, U., & Schwarz, H. E. 2001, *ApJ*, 553, 211  
 Damiani, F., Maggio, A., Micela, G., & Sciortino, S. 1997a, *ApJ*, 483, 350  
 Damiani, F., Maggio, A., Micela, G., & Sciortino, S. 1997b, *ApJ*, 483, 370  
 Galloway, D. K. & Sokoloski, J. L. 2004, *ApJ*, 613, L61  
 Groenewegen, M. A. T. & Lamers, H. J. G. L. M. 1989, *A&AS*, 79, 359  
 Gromadzki, M. & Mikołajewska, J. 2009, *A&A*, 495, 931  
 Jeffries, R. D. & Stevens, I. R. 1996, *MNRAS*, 279, 180  
 Jorissen, A., Začs, L., Udry, S., Lindgren, H., & Musaev, F. A. 2005, *A&A*, 441, 1135  
 Lee, H.-W. 2000, *ApJ*, 541, L25  
 Luna, G. J. M. & Costa, R. D. D. 2005, *A&A*, 435, 1087  
 Luna, G. J. M., Sokoloski, J. L., Mukai, K., & Nelson, T. 2013, *A&A*, 559, A6  
 Mikołajewska, J., Acker, A., & Stenholm, B. 1997, *A&A*, 327, 191  
 Montez, Jr., R., Kastner, J. H., & Sahai, R. 2006, in *Bulletin of the American Astronomical Society*, Vol. 38, American Astronomical Society Meeting Abstracts, 1029  
 Mürset, U., Wolff, B., & Jordan, S. 1997, *A&A*, 319, 201  
 Munari, U., Tomov, T., Yudin, B. F., et al. 2001, *A&A*, 369, L1  
 Mürset, U. & Schmid, H. M. 1999, *A&AS*, 137, 473

- Nichols, J. S., DePasquale, J., Kellogg, E., et al. 2007, *ApJ*, 660, 651  
 Ochsenein, F., Bauer, P., & Marcout, J. 2000, *A&AS*, 143, 23  
 Pereira, C. B., Smith, V. V., & Cunha, K. 2005, *A&A*, 429, 993  
 Protassov, R., van Dyk, D. A., Connors, A., Kashyap, V. L., & Siemiginowska, A. 2002, *ApJ*, 571, 545  
 Santander-García, M., Corradi, R. L. M., Mampaso, A., et al. 2008, *A&A*, 485, 117  
 Schmid, H. M., Kaufer, A., Camenzind, M., et al. 2001, *A&A*, 377, 206  
 Schmid, H. M. & Nussbaumer, H. 1993, *A&A*, 268, 159  
 Schwarz, H. E., Aspin, C., & Lutz, J. H. 1989, *ApJ*, 344, L29  
 Sekeráš, M. & Skopal, A. 2012a, *Baltic Astronomy*, 21, 196  
 Sekeráš, M. & Skopal, A. 2012b, *MNRAS*, 427, 979  
 Smith, V. V., Pereira, C. B., & Cunha, K. 2001, *ApJ*, 556, L55  
 Soker, N. & Kastner, J. H. 2003, *ApJ*, 583, 368  
 Stute, M. & Sahai, R. 2009, *A&A*, 498, 209  
 van den Heuvel, E. P. J. & Bonsema, P. T. J. 1984, *A&A*, 139, L16  
 Webster, B. L. & Allen, D. A. 1975, *MNRAS*, 171, 171  
 Whitelock, P. A. & Munari, U. 1992, *A&A*, 255, 171

<sup>1</sup> <http://heasarc.gsfc.nasa.gov/docs/archive.html>

<sup>2</sup> Offset from instrument aim point, obtained from HEASARC

<sup>3</sup> <http://cxc.cfa.harvard.edu/ciao/index.html>

<sup>4</sup> <http://simbad.u-strasbg.fr/simbad/sim-fid>

<sup>5</sup> <http://heasarc.gsfc.nasa.gov/docs/xanadu/xspec/>

<sup>6</sup> <http://www.nustar.caltech.edu/>

<sup>7</sup> <http://www.mpe.mpg.de/eROSITA>